



The correlation between electrical properties and surface plasmonic properties on ITO films with diffraction grating

Noriyuki Hasuike¹ · Nobutoshi Miyamoto¹ · Kohei Funahashi¹ · Minoru Takeda¹

Received: 8 April 2021 / Accepted: 19 July 2021 / Published online: 2 August 2021
© The Optical Society of Japan 2021

Abstract

The correlation between electrical properties and surface plasmon resonance (SPR) wavelength was discussed using ITO grating coupler. ITO films were prepared on SiO₂/Si substrate by RF sputtering with thermal annealing, and the grating was directly fabricated on the sample surface by focused ion beam. Electron density and mobility were evaluated by fitting optical reflection spectra according to Drude model, and then SPR wavelength was estimated from the dispersion relation of surface plasmon. Characteristic SPR dip was observed in polarized reflection spectrum, however, measured wavelength was different from theoretically estimated value. The discrepancy was explained by introducing the assumption based on effective medium theory, in which the grating is assumed as a thin film with effective refractive index.

Keywords Surface plasmon resonance · ITO · Grating coupler · Effective medium theory

1 Introduction

Indium tin oxide (ITO) has been expected as one of candidates for plasmonic materials working at infrared (IR) spectral region [1–4]. The correlation between carrier density and optical properties, which is caused by local surface plasmon polaritons (LSPPs), has been discussed in dopant-controlled ITO nanocrystals [5, 6]. In particular, ITO nanoparticle films showed interesting optical properties such as wavelength selective reflection and transmission for electromagnetic waves longer than IR light, which depends on the particle size and the gap between particles [7]. It is greatly expected to be applied to smart-window technology, in which both heat-shielding effect due to IR reflection and microwave transmission for wireless communications are simultaneously realized.

On the other hand, propagating surface plasmon polaritons (SPPs) has also been attracted much attention, which are coupled with incident light and propagates over long

distances along the surface without reradiation of the light. A number of studies have focused on the optical properties of propagating SPPs on metal surface such as Au and Ag. For example, metal thin films with periodic surface nanostructure have been devised that can achieve both functions of a bandpass filter and focusing lens with small spot size exceeding the diffraction limit of light at the same time [8–10].

For propagating SPPs on ITO, fundamental optical properties have been studied using Kletchmann arrangement [1, 11, 12]. It is well known that the relationship between SPP frequency and the wavenumber depends on complex dielectric constant of both the material and adjacent medium. In case of ITO, complex dielectric constant can be modulated by varying the electrical properties such as electron density and mobility, because they are affected by oxygen vacancies and Sn doping level [13–15]. This means that plasmonic properties of ITO can be tuned by the electrical properties under same nanostructure and excitation condition. This gives a significant advantage for device application.

We have studied on the excitation of propagating SPPs via ITO grating coupler, and clarified the relationship between surface plasmon resonant (SPR) wavelength and the grating pitch [16]. In this study, we discuss the correlation between

✉ Noriyuki Hasuike
hasuike@kit.ac.jp

¹ Department of Electronics, Kyoto Institute of Technology,
Matsugasaki, Sakyo-ku, Kyoto 606-8585, Japan

SPR wavelength and electrical properties via ITO grating coupler.

2 Experimental methods

ITO film with thickness of 600 nm was deposited on SiO₂ (100 nm)/Si substrate at 300 °C by RF sputtering method. Ar gas was conducted to the sputtering chamber as a sputtering gas and the pressure was maintained at 3 mTorr during sputtering process. In₂O₃-SnO₂(90:10 wt%) ceramics was used as a sputtering target and 100 W RF power was applied to the target. Two kinds of ITO films were prepared; One is as-sputtered sample (sample 1) and the other is the sample annealed at 500 °C for 2 h in vacuum after sputtering deposition (sample 2).

Electrical properties such as electron density and mobility were evaluated by fitting optical reflection spectra according to Drude model. The procedure is described in detail in next section.

The grating with 1 μm pitch was directly fabricated on ITO surface using focused ion beam (FIB) method. The pitch and the depth were observed by optical microscope and scanning electron microscope (SEM).

The optical reflection measurement was carried out to evaluate SPR wavelength with microspectrophotometer. Polarized incoming light was incident normal to the grating using Cassegrain reflector lens with NA = 0.57, and the irradiation area was limited with 50 μmΦ aperture to fit the grating area.

3 Results and discussion

3.1 Drude fitting analysis

The behavior of free electron in ITO is described properly according to Drude model, and in which electrical properties can be evaluated by fitting the optical reflection spectrum [17]. Reflectance is given by following equation using complex refractive index $\tilde{n} = n(\omega) + i\kappa(\omega)$;

$$R(\omega) = \left| \frac{\tilde{n}(\omega) - 1}{\tilde{n}(\omega) + 1} \right|^2 = \frac{\{n(\omega) - 1\}^2 + \kappa(\omega)^2}{\{n(\omega) + 1\}^2 + \kappa(\omega)^2} \tag{1}$$

where $n(\omega)$ and $\kappa(\omega)$ is refractive index and extinction coefficient, respectively. And, following relationship also holds between complex dielectric constant of $\tilde{\epsilon}(\omega) = \epsilon_1(\omega) + i\epsilon_2(\omega)$ and $\tilde{n}(\omega)$;

$$\epsilon_1 = n^2 - k^2 \tag{2}$$

$$\epsilon_2 = 2nk \tag{3}$$

and

$$n = \frac{1}{\sqrt{2}} \left\{ \epsilon_1 + (\epsilon_1^2 + \epsilon_2^2)^{\frac{1}{2}} \right\}^{\frac{1}{2}} \tag{4}$$

$$k = \frac{1}{\sqrt{2}} \left\{ -\epsilon_1 + (\epsilon_1^2 + \epsilon_2^2)^{\frac{1}{2}} \right\}^{\frac{1}{2}} \tag{5}$$

Complex dielectric constant of ITO $\tilde{\epsilon}_{ITO}(\omega)$ can be given by following equation based on Drude model;

$$\tilde{\epsilon}_{ITO}(\omega) = \epsilon_{opt} \left\{ 1 - \frac{\omega_p^2}{(\omega^2 + i\Gamma\omega)} \right\} \tag{6}$$

where ϵ_{opt} and Γ are optical dielectric constant and damping constant, respectively [18]. And, ω_p is called plasma frequency and given by following equation;

$$\omega_p = \left(\frac{Ne^2}{\epsilon_{opt}\epsilon_0 m^* m_0} \right)^{\frac{1}{2}} \tag{7}$$

where N , e , ϵ_0 , m^* and m_0 are electron density, elementary charge of electron, permittivity of free space, electron effective mass and electron rest mass, respectively. According to above relationships, optical reflection spectra can be analyzed using ω_p and Γ as fitting parameters and the electron density N can be evaluated. The mobility μ can be calculated from following equation:

$$\mu = \frac{e}{m^* m_0 \Gamma} \tag{8}$$

Figure 1 shows optical reflection spectra of the samples, and experimental data are indicated by solid line.

The spectra showed clear plasma reflection edge around 1200 nm, where the reflectance increased sharply. Drude fitting analysis was applied to the spectra to evaluate the electrical properties. Here, optical dielectric constant $\epsilon_{opt} = 4.4$ and effective mass $m^* = 0.4 m_0$ were used for the fitting analysis [17, 19]. The fitted curves are indicated by dotted line in the figure, and the result showed good agreement with the experimental spectra. Subsequently, the electron density N and the mobility μ were calculated from ω_p and Γ , and obtained values are summarized in Table 1.

Comparing the values, it is confirmed that the electron density increased and the mobility decreased by annealing. This is because oxygen vacancies were introduced and simultaneously acted as donors and ionized impurities, contributing to increase and decrease in the electron density and the mobility.

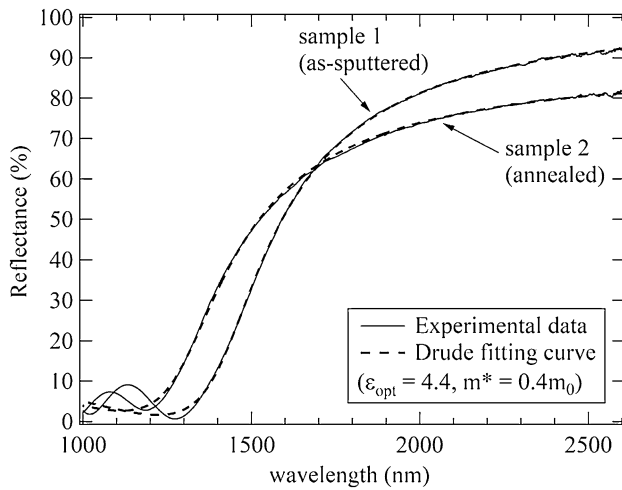


Fig. 1 Optical reflection spectra of the samples. Experimental and Drude fitting curve are shown by solid and dotted line, respectively

3.2 Fabrication of grating

The grating was fabricated directly on ITO surface using FIB method. 50 grooves with 1 μm pitch were fabricated in the

area of $50 \times 100 \mu\text{m}$ as designed value for processing. For sample 1, optical micrograph and top view of SEM image are shown in figure 2(a) and (b), respectively.

The pitch Λ and the duty cycle ($= a/\Lambda$) are estimated roughly at 1.0 μm and 45 %, respectively. In addition, the cross-section was exposed by FIB processing to observe the shape and the depth of the grating, and SEM observation was carried out with the sample tilted 45 $^\circ$ as shown in figure 2(c). The grating had rectangular shape with slightly rounded corners and the depth d was estimated around 200 nm. And, hemispherical morphologies were observed on the grating surface, which represents the surface roughness of ITO film. The observation was conducted for sample 2 in a same manner, and measured values are summarized in Table 2. Figure 2(d) shows the schematic diagram of the grating.

3.3 Polarized reflection spectroscopy

Polarized optical reflection measurement was carried out to evaluate SPR wavelength. It is well known that SPP excitation via grating couplers can be achieved by the incident of polarized light. The component of the wavevector of

Table 1 Drude fitting parameter and calculated electrical properties

	Drude fitting parameter		Electrical properties	
	Plasma freq.	Damp. const.	Elec. dens.	Mobility
	ω_p (nm)	Γ (fs)	N (cm^{-3})	μ ($\text{cm}^2/(\text{V}\cdot\text{s})$)
Sample 1 (as-sputtered)	1420	26.7	9.7×10^{20}	18.7
Sample 2 (annealed)	1300	22.1	1.2×10^{21}	15.4

Fig. 2 Optical micrograph (a), top view of SEM image (b), cross sectional view of SEM image (c) and schematic diagram of the diffraction grating (d)

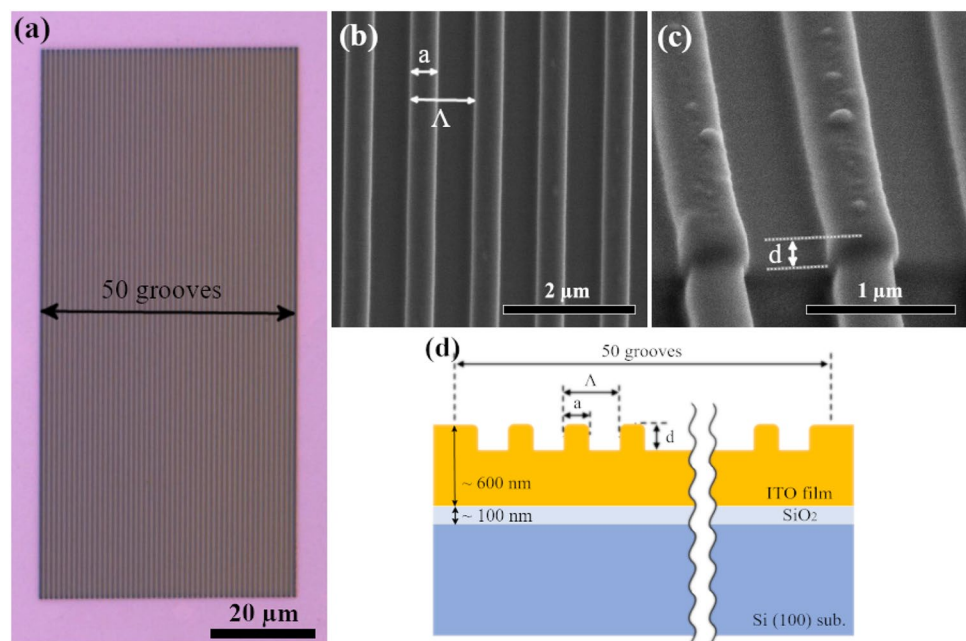


Table 2 The structure of the grating, and measured and calculated SPR wavelength

	Grating structure			SPR wavelength	
	Pitch	Duty cycle	Depth	Exp.	Calc.
	$\Lambda(\mu\text{m})$	a/Λ (%)	d (nm)	(nm)	(nm)
Sample 1 (as-sputtered)	1.0	45	~ 200	2080	1655
Sample 2 (annealed)	1.0	34	~ 200	1830	1536

diffracted light parallel to the interface can be matched to that of SPP waves. Consequently, decrease in reflectance appears as a characteristic dip in the spectrum at SPR wavelength. In this study, the polarization direction was defined as shown in figure 3(a), that is, *p*- and *s*-polarized incident light have electric field vector parallel and normal to the grating vector, respectively.

Figure 3(b), (c) shows polarized reflection spectra for the samples. In each sample, *p*-polarized spectrum had broad dip in reflectance at the wavelength indicated by downward arrow in the figure. The wavelengths were roughly estimated at 2080 nm and 1830 nm for each sample, and this is the spectral evidence of SPP excitation. The validity of these values will be discussed in the next section in terms of SPP dispersion relation.

In addition, the followings were also confirmed in common for both samples; first, plasma reflection edge was shifted to longer wavelength side in both *p*- and *s*-polarized spectra than that of flat surface. Second, the reflectance was decreased in *s*-polarized spectra than that of flat surface on longer wavelength side from plasma edge, and it became more pronounced in *p*-polarized spectra. These features are explained by introducing the assumption called effective medium theory (EMT) that the grating layer behaves as a

thin film with effective refractive index and it also has optically anisotropic [21]. It means that ITO grating can exhibit different reflectance depending on the polarization direction. These phenomena have been discussed in subwavelength structure (SWS) [20], and details will be discussed in the next section.

3.4 SPP dispersion relation

When SPP is excited at the interface between two kinds of medium having complex dielectric constant $\tilde{\epsilon}_1$ and $\tilde{\epsilon}_2$, the dispersion relation between SPP frequency ω_{SPP} and SPP wavenumber k_{SPP} is given by following equation:

$$k_{SPP} = \frac{\omega_{SPP}}{c} \left\{ \frac{\tilde{\epsilon}_1 \cdot \tilde{\epsilon}_2}{\tilde{\epsilon}_1 + \tilde{\epsilon}_2} \right\}^{\frac{1}{2}} \tag{9}$$

For SPP excited at the interface between ITO and air, the formula can be rewritten as follows using the complex dielectric constant of ITO ($\tilde{\epsilon}_{ITO} = \epsilon'_{ITO} + i\epsilon''_{ITO}$) and air ($\tilde{\epsilon}_{air} = 1$);

$$k_{SPP} = \frac{\omega_{SPP}}{c} \left(\frac{\epsilon'_{ITO}}{\epsilon'_{ITO} + 1} \right)^{\frac{1}{2}} \tag{10}$$

According to eq. (6), ϵ'_{ITO} is given by Drude model as follows.

$$\epsilon'_{ITO} = \epsilon_{opt} \left(1 - \frac{\omega_p^2}{\omega^2 + \Gamma^2} \right) \tag{11}$$

From these equations, the dispersion relation can be calculated with ω_p and Γ .

Figure 4(a) shows dispersion curves calculated using the values shown in Table 1. Note that Γ was set to 0 in

Fig. 3 Schematic diagram of the polarization direction of the incident light (a). The direction of electric field vector are shown by black solid arrows. Polarized reflection spectra for the sample 1 (b) and 2 (c)

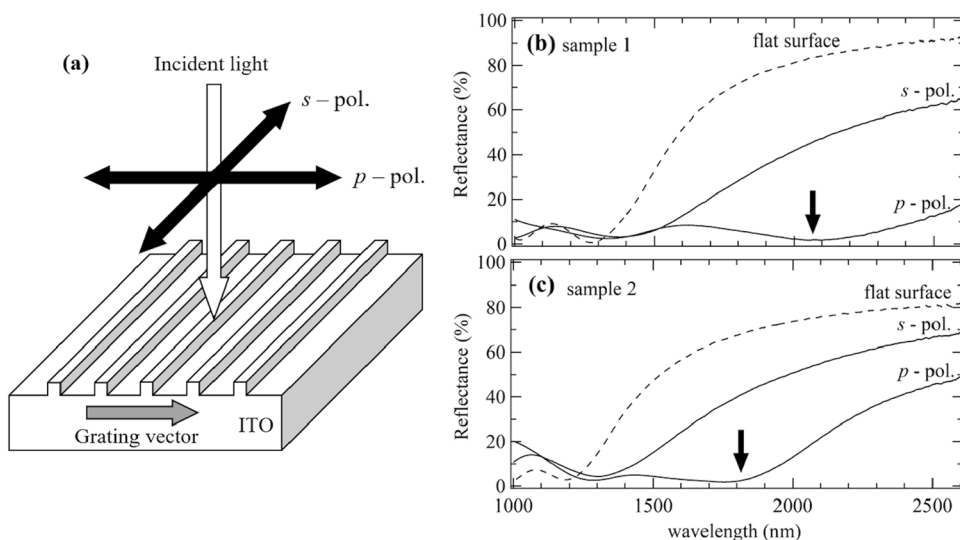
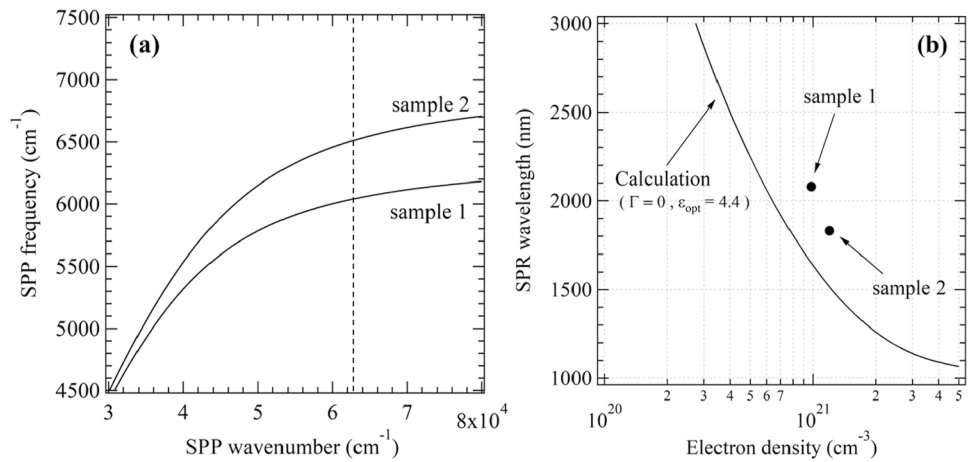


Fig. 4 Calculated dispersion curves (a), and calculated SPR wavelength depending on electron density (b). Experimental data are indicated by black dots



consideration of undamped ideal propagating SPP. When *p*-polarized light is incident normal to the grating, SPP waves having wavenumber k_{SPP} can be coupled to the wavevector equal to grating vector $|K| = 2\pi/\Lambda$, where Λ is the grating pitch. That is, ω_{SPP} is given at the point of $k_{SPP} = |K| = 2\pi/\Lambda$ on the dispersion curve. In Fig. 4(a), k_{SPP} is indicated by dotted line, and it was clearly confirmed that sample 2 had higher ω_{SPP} than that of sample 1.

Figure 4(b) shows SPR wavelength expected from the above concepts as a function of the electron density *N*.

The figure also contains experimental data indicated by black dots. Both the experimental and estimated values tended to shift to shorter wavelength, but there was a slight difference between them. The discrepancy is explained by taking into account the assumption based on EMT mentioned in Sect. 3.3.

When the incident light has longer wavelength than the grating pitch, the grating operates as SWS. As shown in Fig. 5(a) and (b), it is convenient to assume the grating as an optically anisotropic thin film with the effective refractive

indices n_s and n_p for *s*- and *p*-polarization. These values are calculated using the refractive indices of adjacent mediums and filling factor $f = a/\Lambda$ of the grating[20]. Note that when the material of the grating is metal, EMT is not valid due to large complex value of dielectric constant. In our case, however, since complex value of ITO is smaller than that of metals such as gold and silver, light waves can penetrate into ITO bulk to a certain depth. Therefore, the grating layer is assumed to ITO thin film with no plasmonic absorption and imaginary part of complex dielectric constant is approximated to zero to simplify the calculation. According to this assumption, SPP dispersion relation between ITO thin film and underlying bulk ITO was calculated as a function of filling factor *f*.

Figure 5(c) shows calculated dispersion curves for sample 1. The curve shifted depending on *f* values, that is, SPR frequency was varied by changing *f* value. Figure 5(d) shows estimated SPR wavelength as a function of *f*, and experimental data are also indicated by black dots. The results clearly presented good agreement between experimental and

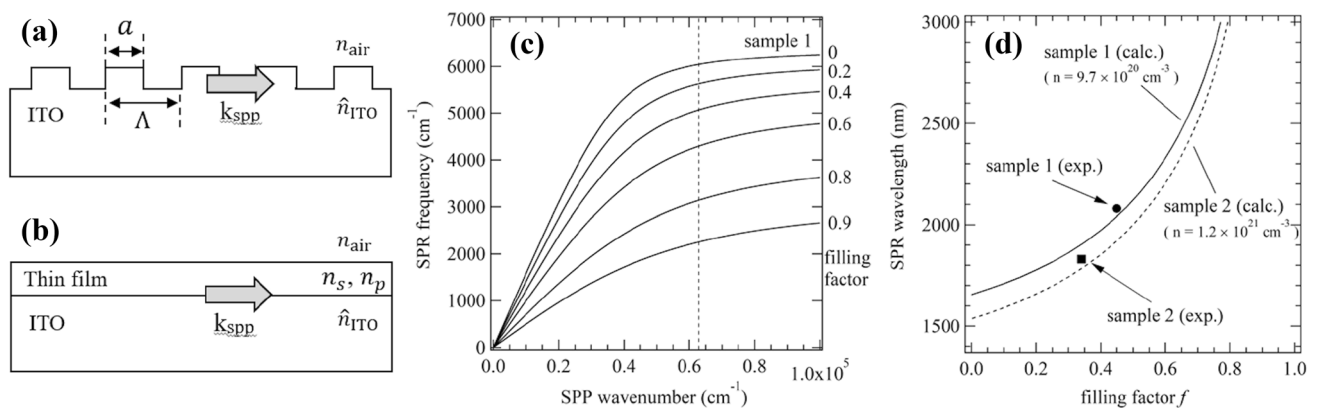


Fig. 5 Schematic diagram of ITO grating (a) and ITO thin film assumed by EMT (b). The dispersion curves calculated using filling factor *f* for sample 1 (c), and estimated SPR wavelength and experimental data as a function of *f* (d)

estimated values, suggesting that the assumption based on EMT can predict successfully SPR wavelength in ITO grating coupler.

4 Conclusion

We discussed the correlation between electrical properties and SPR wavelength via ITO grating couplers. Characteristic dip caused by SPP excitation was observed on *p*-polarized reflection spectrum, however, experimental values were different from the values expected from SPP dispersion relation. The discrepancy could be successfully explained by introducing the assumption that assumes the grating as a thin film with effective refractive index.

References

- Rhodes, C., Franzen, S., Maria, J.-P., Losego, M., Leonard, D.N., Laughlin, B., Duscher, G., Weibel, S.: Surface plasmon resonance in conducting metal oxides. *J. Appl. Phys.* **100**(5), 054905 (2006)
- West, P.R., Ishii, S., Naik, G.V., Emani, N.K., Shalae, V.M., Boltasseva, A.: Searching for better plasmonic materials. *Laser Photo. Rev.* **4**, 795 (2010)
- Li, S.Q., Guo, P., Zhang, L., Zhou, W., Odom, T.W., Seideman, T., Ketterson, J.B., Chang, R.P.H.: Infrared plasmonics with indium-tin-oxide nanorod arrays. *ACS Nano* **5**, 9161 (2011)
- Dao, T.D., Doan, A.T., Ngo, D.H., Chen, K., Ishii, S., Tamanai, A., Nagao, T.: Selective thermal emitters with infrared plasmonic indium tin oxide working in the atmosphere. *Opt. Mater. Exp.* **9**, 2534 (2019)
- Matsui, H., Furuta, S., Tabata, H.: Role of electron carriers on local surface plasmon resonances in doped oxide semiconductor nanocrystals. *Appl. Phys. Lett.* **104**, 211903 (2014)
- Kanehara, M., Koike, H., Yoshinaga, T., Teranishi, T.: Indium tin oxide nanoparticles with compositionally tunable surface plasmon resonance frequencies in the near-IR region. *J. Am. Chem. Soc.* **131**, 17736 (2009)
- Matsui, H., Hasebe, T., Hasuike, N., Tabata, H.: Plasmonic heat shielding in the infrared range using oxide semiconductor nanoparticles based on Sn-Doped In_2O_3 : effect of size and interparticle gap. *ACS Appl. Nano Mater.* **1**, 1853 (2018)
- Livneh, N., Harats, M.G., Istrati, D., Eisenberg, H.S., Rapaport, R.: Highly directional room-temperature single photon device. *Nano Lett.* **16**, 2527 (2016)
- Yamaguchi, K., Yamanaka, H., Ohtsu, T., Ishii, S.: Electrically driven plasmon chip: active plasmon lens in the visible range. *Appl. Phys. Lett.* **108**(11), 111903 (2016)
- Andersen, S.K.H., Bogdanov, S., Makarova, O., Xuan, Y., Shalaginov, M.Y., Boltasseva, A., Bozhevolny, S.I., Shalae, V.M.: Hybrid plasmonic bullseye antennas for efficient photon collection. *ACS Photo.* **5**, 692 (2018)
- Rhodes, C., Cerruti, M., Efremenko, A., Losego, M., Aspnes, D.E., Maria, J.-P., Franzen, S.: Dependence of plasmon polaritons on the thickness of indium tin oxide thin films. *J. Appl. Phys.* **103**(9), 093108 (2008)
- Losego, M.D., Efremenko, A.Y., Rhodes, C.L., Cerruti, M.G., Franzen, S., Maria, J.-P.: Conductive oxide thin films: model systems for understanding and controlling surface plasmon resonance. *J. Appl. Phys.* **106**(2), 024903 (2009)
- Kimura, H., Watanabe, H., Ishihara, S., Suzuki, Y., Ito, T.: DC magnetron sputtered ITO films applied with indium tin oxide targets. *Shinku* **30**(6), 546–554 (1986)
- Utsumi, K., Iigusa, H.: The effect of SnO_2 concentration of the electrical and optical properties of In_2O_3 - SnO_2 films TOSOH res. *Tech. Rev.* **47**, 11 (2003)
- Haranou, T., Takaki, S.: A review of typical properties of indium-tin oxide films. *Hyohmen-Gijyutu* **40**, 666 (1989)
- Hasuike, N., Ochiai, S., Iwakiri, R., Takeda, M., Yoo, W.S., Isshiki, T.: Surface plasmon resonances in Sn: In_2O_3 . *Thin Films Diff. Grating Proc.* **2**, 1034 (2018)
- Wolf, N., Gerstenlauer, D., Manara, J.: Modelling the spectral reflectances of miscellaneous ITO coating by using only the Drude theory. *J. Phys. Conf. Series* **395**, 012064 (2012)
- Fox, M.: *Optical properties of solids*, 2nd edn. Oxford Univ Pr (2010)
- Ohhata, Y., Shinoki, F., Yoshida, S.: Optical properties of rf reactive sputtered thin-doped In_2O_3 films. *Thin Solid Films* **59**, 255 (1979)
- Kikuta, H., Toyota, H., Yu, W.: Optical elements with subwavelength structured surfaces. *Opt. Rev.* **10**, 63 (2003)
- Rytov, S.M.: Electromagnetic properties of a finely stratified medium. *Soviet Phys. JETP* **2**, 466 (1956)

Publisher's Note Springer Nature remains neutral with regard to jurisdictional claims in published maps and institutional affiliations.